



Valorization of lignin from pine (*Pinus* spp.) residual sawdust: antioxidant activity and application in the green synthesis of silver nanoparticles for antibacterial purpose

Matheus Cavali¹ · Carlos Ricardo Soccol² · Débora Tavares² · Luis Alberto Zevallos Torres² · Valcineide Oliveira de Andrade Tanobe² · Arion Zandoná Filho³ · Adenise Lorenci Woiciechowski²

Received: 28 May 2021 / Revised: 31 August 2021 / Accepted: 8 September 2021 / Published online: 27 September 2021
© The Author(s), under exclusive licence to Springer-Verlag GmbH Germany, part of Springer Nature 2021

Abstract

Lignin is the second most abundant biopolymer available whose functional groups make it a natural antioxidant. Pine residual sawdust is a lignocellulosic waste largely produced in sawmills by wood processing. Thus, this study aimed to evaluate the lignin from pine residual sawdust (PRSL) as an environmental-friendly antioxidant, and in the green synthesis of silver nanoparticles (LAgNPs), which were then tested against Gram-positive and Gram-negative bacteria. Three PRSL, previously obtained by sequential acid-alkaline treatment at 130, 150, and 170 °C, were assessed. The total phenolic content (TPC) and antioxidant activity of PRSL were also evaluated. PRSL showed strong potential as a natural antioxidant. LAgNPs were characterized by Fourier-transform infrared spectroscopy (FTIR), dynamic light scattering (DLS), and transmission electron microscopy (TEM). LAgNPs presented a polydispersed mixture with an average diameter of 54.18 nm and efficient antibacterial properties. Therefore, this study demonstrated the great capability of PRSL as a natural antioxidant agent and for green synthesis of silver nanoparticles.

Keywords Lignin · Sawdust · Antioxidants · Green synthesis · Nanoparticles · Antibacterial

1 Introduction

Cellulose and hemicellulose comprise the main fractions of biomass along with lignin, which is the second most abundant biopolymer [1]. Lignin is available either as transformed lignin through industrial separation processes or as native lignin in plants, presenting great potential as raw material for the production of chemicals [2, 3]. It presents organic functional groups, such as phenolic, alcoholic, carbonyl, carboxyl, and methoxyl, which play an important role

in the stabilization of reactions induced by oxygen radicals and their derived species, making lignin a promising antioxidant agent [4, 5]. Therewithal, there are large markets for antioxidant applications, such as biodiesel, rubber, and plastic industries [6–9]. These opportunities foster researches regarding lignin as a natural and environment-friendly antioxidant.

The antioxidant properties of lignin are influenced by its source as well as the recovery method used [10, 11]. Many studies about the antioxidant activity of lignin from different sources, such as rice straw, apple tree pruning residues, sugarcane bagasse, oil palm empty fruit bunches, and wheat straw, have been reported [12–16]. However, little attention has been paid to the antioxidant properties of lignin extracted from pine residual sawdust.

The use of lignocellulosic wastes as source of lignin is considerably advantageous because it contributes adding value to the residues and promoting environmental-friendly processes [17]. For instance, pine residual sawdust is a waste generated in large quantities in the pine (*Pinus* spp.) industry [18]. At sawmills, only approximately 45–65% of the raw material is recovered during the wood mechanical

✉ Adenise Lorenci Woiciechowski
adeniselw@gmail.com

¹ Department of Sanitary and Environmental Engineering, Federal University of Santa Catarina, Florianópolis 88040-970, Santa Catarina, Brazil

² Department of Bioprocess Engineering and Biotechnology, Federal University of Paraná, Centro Politécnico, CP 19011, Curitiba 81531-908, Paraná, Brazil

³ Department of Chemical Engineering, Federal University of Paraná, Centro Politécnico, CP 19011, Curitiba 81531-908, Paraná, Brazil

processing [19, 20]. Brazilian timber industry annually produces around 48.1 million m³ of wastes from mechanical processes, comprising of bark, slabs, chips, and sawdust [21]. The European Organization of the Sawmill Industry, where softwood is the main feedstock used, revealed that the sawdust production in 2020 was 12.8 million m³, and it estimates that the production in 2021 will be almost 13.2 million m³ [22]. Hence, that amount of residual sawdust might be an environmental concern if disposed of improperly [23].

Lignin has also been investigated in the nanotechnology field for the synthesis of metallic nanoparticles. These nanostructures have received plenty attention in diverse fields, such as environment [24], catalysis [25], dermatology and cosmetology [26], food packaging [27], and biomedical applications [28], among others [29]. Synthesis of silver nanoparticles can be performed by physical methods, such as laser ablation and evaporation–condensation, chemical methods that make use of organic and inorganic reducing agents, and biological methods, which use natural reducing agents [29, 30]. However, although physical and chemical methods are able to effectively synthesize pure and well-defined nanoparticles, the former produces lower amounts of silver nanoparticles, while the latter consumes a lot of energy and employs toxic reagents [30]. Therefore, the development of processes free of harmful reagents, to expand the nanotechnology field in an environmentally friendly way, is necessary. As an alternative, biological methods consist of applying molecules obtained from living organisms, such as microorganisms [31], plants [32–34], agricultural wastes, enzymes, and pigments [35, 36], as reducing and stabilizing agents [37].

Recently, the combination of different biomasses (pine sawdust, bagasse, lignin, and cellulose) and their corresponding biochars were tested in the synthesis of silver nanoparticles due to the redox reactive –OH groups of biomass and biochar [38]. Regarding lignin, the green synthesis of silver nanoparticles using this biopolymer has been proved to be convenient [2, 39, 40]. Lignin presents multiple functional groups with the potential to reduce silver ions into silver nanoparticles [2, 36]. As a natural and abundant resource, lignin can serve not only as reducing but also as stabilizing agent for synthesizing silver nanoparticles [39]. Moreover, silver nanoparticles have been suggested for important applications, such as antibacterial, larvicidal, pupicidal, antioxidant, and anticoagulant [34, 41–43]. Additionally, lignin-mediated silver nanoparticles have also shown antimicrobial capacities attributed to the presence of silver, which is known for its antiseptic effect on microorganisms [44, 45].

Accordingly, this study aimed to assess the antioxidant activity of lignin extracted from pine residual sawdust as well as its application in the green synthesis of lignin-mediated silver nanoparticles (LAGNPs). Furthermore, the

antibacterial properties of LAGNPs were evaluated against Gram-positive and Gram-negative bacteria.

2 Material and methods

Pine residual sawdust lignin (PRSL) was extracted and recovered from *Pinus* spp. as described in another research [17] by sequential acid-alkaline treatment at different temperatures (130, 150, and 170 °C). Three different recovered lignins, named PRSL-130, PRSL-150, and PRSL-170, were used in the following experiments. Previously, the lignin samples were washed with ultrapure water and subsequently dried in an air-circulating oven. The antioxidant and antibacterial activities of lignin were assessed using aqueous solutions of lignin samples. The lignin solutions were prepared as described elsewhere with some modifications [15]. Briefly, PRSL-130, PRSL-150, and PRSL-170 were solubilized in alkaline deionized water ($pH = 12$) at 60 °C with magnetic stirring. The lignin solutions were then neutralized ($pH = 7$) using 5% ($v \cdot v^{-1}$) H₂SO₄ to be used in all of the following tests.

2.1 Total phenolic content of PRSL

The total phenolic content (TPC) of PRSL was evaluated by the Folin-Ciocalteu method [15]. Briefly, 500 μ L of lignin solution (200 μ g·mL⁻¹) was mixed with 2.5 mL of 1:10 ($wt \cdot v^{-1}$) Folin-Ciocalteu solution. After 5 min, 2 mL of 7.5% ($wt \cdot v^{-1}$) Na₂CO₃ was added. The final solution rested for 1 h in the dark at room temperature. Subsequently, the solution was analyzed at 740 nm in a spectrophotometer (Spectrumlab 22PC). Deionized water was used as blank, and a standard calibration curve was prepared using gallic acid (C₇H₆O₅) in the range of 0–100 μ g·mL⁻¹. TPC test was carried out in triplicate for each PRSL, and the results were analyzed by analysis of variance (ANOVA). The TPC values were expressed in milligrams (mg) of gallic acid equivalent (GAE) per gram (g) of lignin.

2.2 Antioxidant activity of PRSL

The DPPH (1,1-diphenyl-2-picrylhydrazyl) assay was carried out by mixing 0.2 mL of lignin solution with 0.8 mL of DPPH• radical solution (0.1 mmol·L⁻¹ — dissolved in methanol). After vigorous agitation, the mixture was placed in the dark for 30 min, and the absorbance at 517 nm was recorded (SP-2000 Spectrophotometer). For the control solution, 0.2 mL of water was mixed with 0.8 mL of DPPH• radical solution. The assessed concentrations of lignin were 50, 100, 150, 200, 250, and 300 μ g·mL⁻¹, and the scavenging ability was determined as already reported in literature [15].

The ABTS (2,2'-azino-bis (3-ethylbenzothiazoline-6-sulfonic acid)) assay was performed in microplate [12]. Briefly, 2.0 mL of potassium persulfate ($K_2S_2O_8$) solution ($2.45 \text{ mmol}\cdot\text{L}^{-1}$) was mixed with 2.0 mL of ABTS solution ($7 \text{ mmol}\cdot\text{L}^{-1}$) to generate the radical ABTS• and stored in the dark for 6 h. Then, 50 μL of ABTS• radical solution was added to 200 μL of lignin solutions (5, 7.5, 12.5, 15, 20, 25, 30, 40, and 50 $\mu\text{g}\cdot\text{mL}^{-1}$). After resting for 30 min in the dark, the absorbance was recorded at 734 nm (Power Wave XS). A solution with 50 μL of ABTS• and 200 μL of deionized water was used as control sample. The scavenging ability was calculated as described by the aforementioned studies [12, 15].

The lignin concentration capable of inhibiting 50% of DPPH• and ABTS• radicals (IC_{50}) was estimated. The IC_{50} of both tests were then compared to the IC_{50} of the Trolox® (6-hydroxy-2,5,7,8-tetramethylchroman-2-carboxylic acid), an analog of the vitamin E with high antioxidant properties. All tests were carried out in triplicate, and the results were analyzed by analysis of variance (ANOVA).

2.3 Synthesis of LAgNPs

The synthesis of the LAgNPs was performed as described in other studies [2, 36]. Briefly, PRSL-170 ($200 \mu\text{g}\cdot\text{mL}^{-1}$) and AgNO_3 ($20 \text{ mmol}\cdot\text{L}^{-1}$) solutions were prepared and mixed to obtain final concentrations of $40 \mu\text{g}\cdot\text{mL}^{-1}$ and $2 \text{ mmol}\cdot\text{L}^{-1}$ for PRSL-170 and AgNO_3 , respectively. The synthesis reaction was performed at 80°C for 5 h without agitation and protected from light. Control samples containing only PRSL-170 or AgNO_3 solutions were carried out as well. The kinetics of the synthesis reaction was monitored measuring the absorbance every hour in the range of 200 to 800 nm with a resolution of 1 nm (UV–Vis spectrophotometer – Shimadzu, UV-1601 PC). A quartz cuvette was used in the procedure, and deionized water was used as blank.

2.4 Fourier-transform infrared spectroscopy of LAgNPs

Fourier-transform infrared spectroscopy (FTIR) was carried out in α -ALPHA-R equipment (Bruker), with attenuated total reflectance (ATR) accessory, a resolution of 4 cm^{-1} , 64 scans, and transmittance mode without the elimination of atmospheric compensation. The samples were previously dried overnight at 60°C , and they were then grounded and mixed with potassium bromide (KBr) in a mortar. Finally, the samples were placed in the ATR accessory for acquisition of the corresponding spectra.

2.5 Average size and transmission electron microscopy analysis of LAgNPs

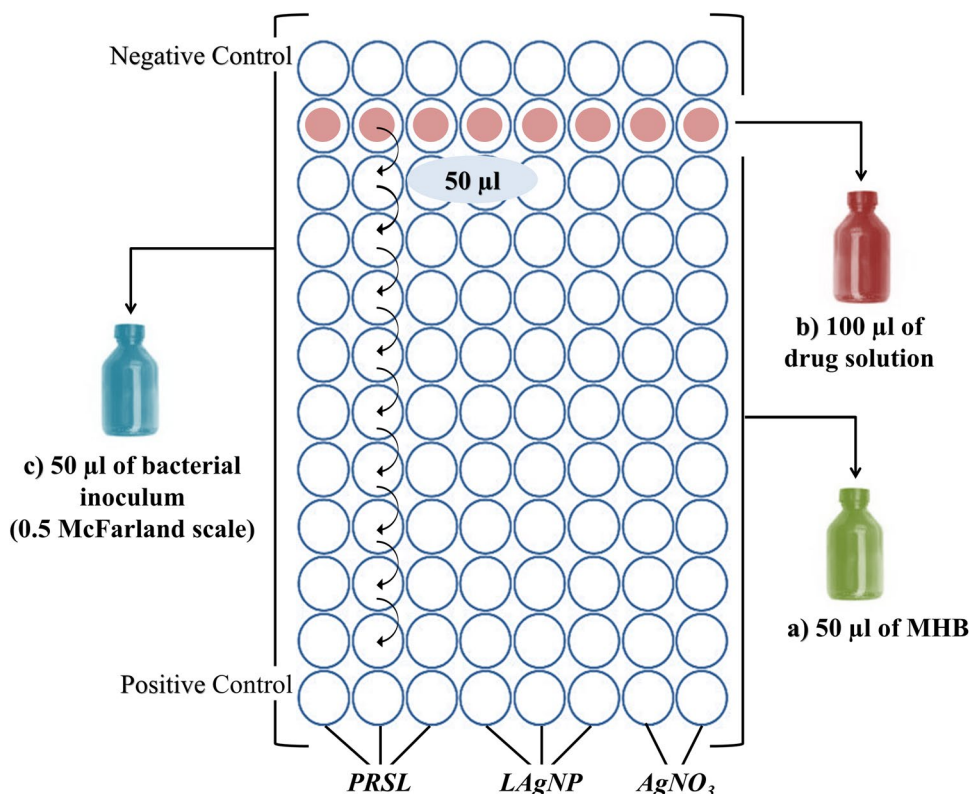
The average size of the LAgNPs was measured by dynamic light scattering (DLS) (Brookhaven, NanoDLS). LAgNPs were also analyzed by a transmission electron microscope (TEM) (JEOL, JEM 1200EX-II) operated at 120 kV to observe their morphology. A drop of the synthesized suspension of LAgNPs was deposited on carbon-coated copper grids, and water was evaporated at room temperature. The selected area electron diffraction (SAED) pattern was analyzed in order to calculate the lattice plane spacings (d-spacings), which were compared to other silver nanoparticles synthesized from plant extracts [33, 46] to verify the silver crystal planes of LAgNPs.

2.6 Antibacterial activity of PRSL and LAgNPs

The antibacterial activity of the PRSL-170 and LAgNPs were evaluated by the broth microdilution method [47] with some modifications. LAgNPs and AgNO_3 solutions were diluted in ultrapure water to the desired initial concentration. The microorganisms used in the test were two Gram-positive (*Staphylococcus aureus* ATCC 29737 and *Bacillus subtilis*) and two Gram-negative (*Escherichia coli* ATCC 25922 and *Salmonella typhimurium* ATCC 14028) strains obtained from the cell bank of the Laboratory of Bioprocess Engineering and Biotechnology of the Federal University of Paraná. Two-fold dilutions of the antibacterial agent were prepared in a Mueller Hinton Broth (MHB) in a 96-well microdilution plate, as depicted in Fig. 1. Initially, 50 μL of MHB (a) was added in every well of the microdilution plate with exception of those on the second row, in which 100 μL of the tested antibacterial solution (b) was added. From each well of the second row, 50 μL was taken and added in the next rows to make serial two-fold dilutions until ten wells were prepared for assessing ten final concentrations of the tested agent. Then, each well was inoculated with 50 μL of the bacterial inoculum (c) that was previously diluted in MHB from a standardized suspension of peptone water (0.1%) adjusted to 0.5 on the McFarland scale.

The AgNO_3 was used in the same concentrations as LAgNPs. Positive and negative growing controls were performed; the former was composed of bacterial inoculum and MHB, and the latter contained only PRSL, LAgNPs, or AgNO_3 solutions mixed with MHB. The microplate was then incubated at 37°C . After 16 h, 30 μL of resazurin ($150 \mu\text{g}\cdot\text{mL}^{-1}$) was added to each well, and the microplate was incubated again for 1 h. Within the viable, metabolic, and active cells, the blue dye resazurin is reduced by oxidoreductase enzymes to resorufin, a pink and fluorescent substance. For that reason, the presence of dark blue color

Fig. 1 Schematic antibacterial evaluation of PRSL and LAgNPs



indicates the inhibitory activity of the antibacterial agent on bacteria at the concentration tested [48–50].

3 Results and discussion

3.1 Total phenolic content

The TPC values, presented in Fig. 2, of PRSL-130, PRSL-150, and PRSL-170, were 226.01 ± 15.60 , 270.16 ± 8.96 , and 247.21 ± 4.03 mgGAE \cdot g $^{-1}$, respectively. The TPC of PRSL-150 was higher than that of PRSL-130, indicating that the increase in the extraction temperature had a proportional effect on the phenolic functional groups of the lignin. However, at higher temperatures (PRSL-170), a reduction of the TPC was observed. This reduction in the TPC at 170 °C might be due to the formation of more condensed structures in lignin that reduces the amount of phenolic hydroxyl groups [51].

According to ANOVA, there were significant differences ($P_{value} < 0.05$) among the TPC of lignin samples, which were attributed to the extraction temperature applied. Treatments performed at high temperatures, strong alkaline conditions, and long reaction times dissolve more components from the lignocellulosic material, producing lignins with higher content of impurities and lower phenolic amounts [5, 52]. The results obtained are in agreement with other studies that

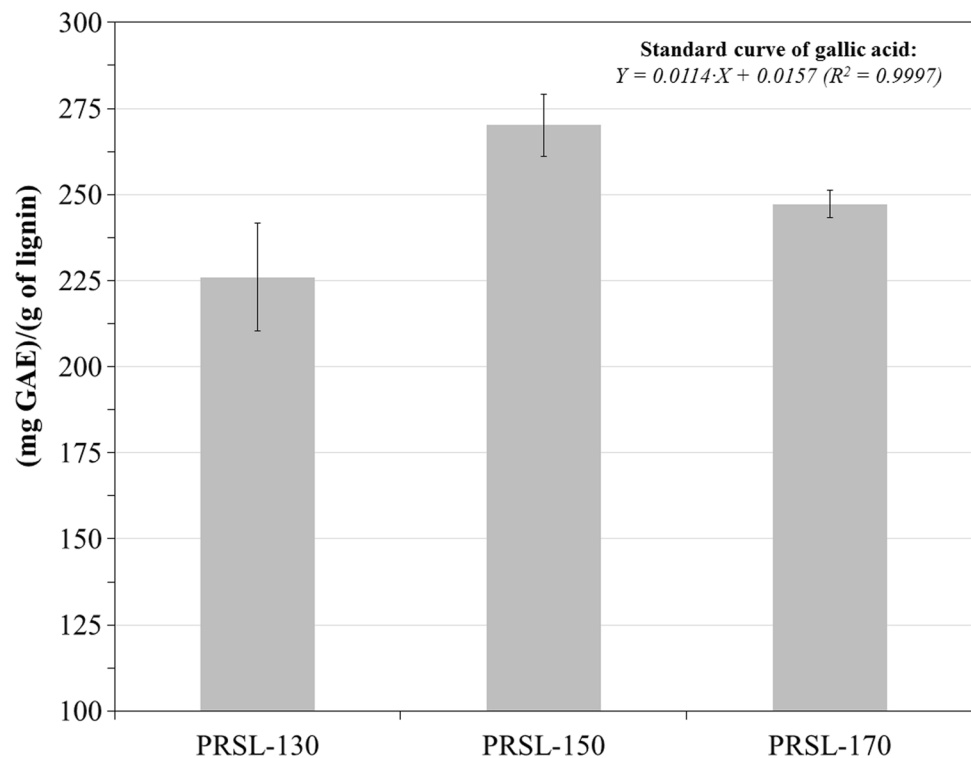
evaluated the TPC of different lignins whose conclusions indicated the content of phenolic hydroxyl groups in lignin was an important factor influencing its antioxidant capacity [5, 10].

3.2 Antioxidant activity of PRSL

The antioxidant activity of PRSL was assessed by evaluating its scavenging potential on DPPH \cdot and ABTS \cdot radicals. Figure 3 shows the antioxidant activity results. It was observed that 250 μ g \cdot mL $^{-1}$ of lignin was necessary to scavenge almost 80% of the DPPH \cdot radicals. In the range of 100 to 300 μ g \cdot mL $^{-1}$, the scavenging activity of PRSL-130, PRSL-150, and PRSL-170 were similar in each concentration tested.

The IC $_{50}$ for the DPPH test was estimated according to logarithm models ($R^2 > 0.96$). The IC $_{50}$ (μ g \cdot mL $^{-1}$) of PRSL-130, PRSL-150, and PRSL-170 were 109.91 ± 2.48 , 92.72 ± 6.16 , and 109.40 ± 2.34 , respectively. PRSL-150 exhibited the lowest IC $_{50}$ among all lignin samples assessed. This result goes in accordance with the TPC test, which revealed that PRSL-150 possessed the highest phenolic hydroxyl content. As stated in other study [10], phenolic hydroxyl groups greatly affect the antioxidant activity of lignin. Besides, lignins with higher quantity of phenolic hydroxyl and methoxy groups present better antioxidative efficiencies [11, 14]. The lignin structure remarkably

Fig. 2 Total phenolic content of PRSL-130, PRSL-150, and PRSL-170, expressed as mg gallic acid equivalent (GAE) per g of lignin



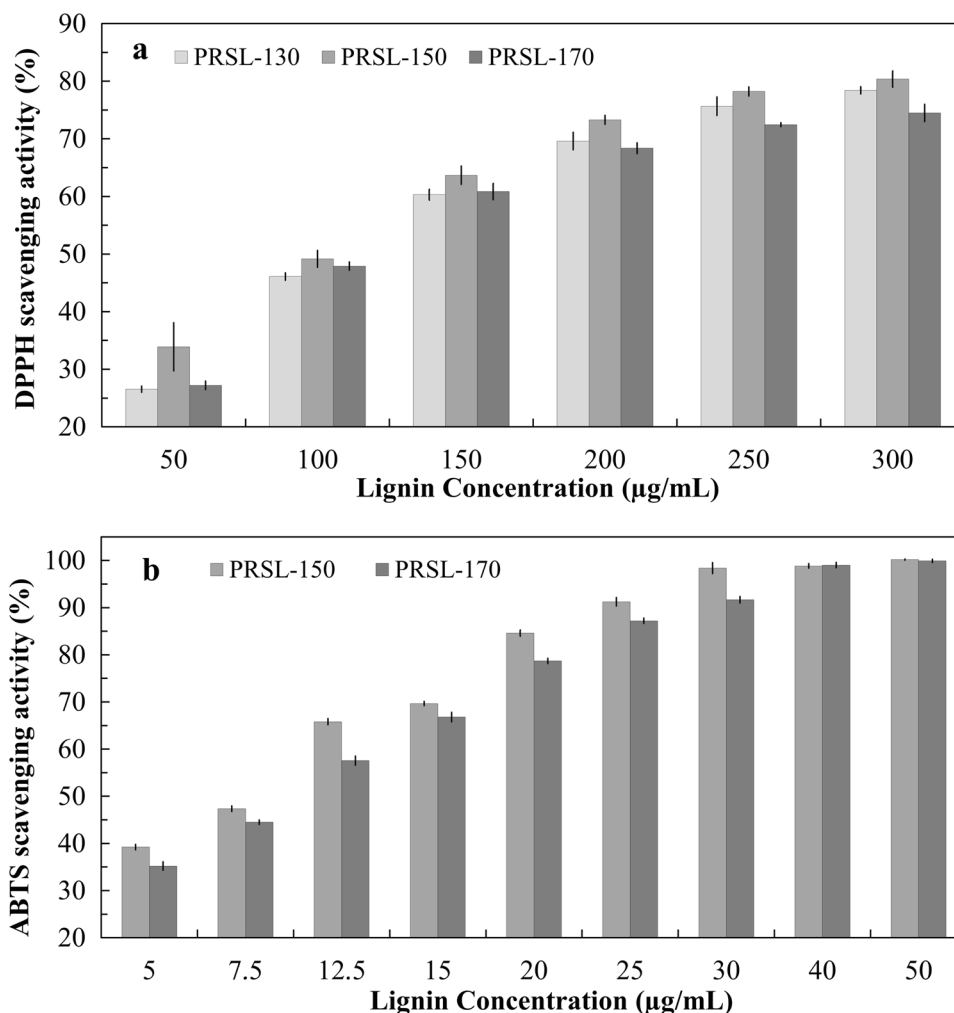
influences on its antioxidant activity, as structural modifications promoted by extraction method alter its bioactivity [12]. Moreover, the presence of non-lignin components such as hemicelluloses could decrease the antioxidant capacity because carbohydrates generate hydrogen bonding with lignin phenolic groups [5]. In a previous study [17], PRSL-150 presented the lowest carbohydrate content on its composition, which explains its slight superior antioxidant capacity, considering the aforementioned effect of carbohydrates on antioxidant properties.

The IC_{50} for PRSL-130 ($109.91 \pm 2.48 \mu\text{g}\cdot\text{mL}^{-1}$) and PRSL-170 ($109.40 \pm 2.34 \mu\text{g}\cdot\text{mL}^{-1}$), obtained from DPPH test, did not present significant difference between them ($P_{value} > 0.05$). However, the yield of the PRSL-170 was higher than PRSL-130 in the lignin recovery process, as previously reported [17]. The specific yields (% — mass of lignin to mass of lignin available in the pretreated pine residual sawdust) achieved at 130, 150, and 170 °C were, respectively, 21.75 ± 0.09 , 44.75 ± 0.52 , and 93.97 ± 0.99 [17]. Additionally, the global yields (% — mass of lignin to mass of pine residual sawdust) were 6.43 ± 0.03 , 13.43 ± 0.16 , and 28.46 ± 0.30 for PRSL-130, PRSL-150, and PRSL-170, respectively. Therefore, only PRSL-170 and PRSL-150 were evaluated in the ABTS test. It was observed that $30 \mu\text{g}\cdot\text{mL}^{-1}$ of PRSL-150 and $40 \mu\text{g}\cdot\text{mL}^{-1}$ of PRSL-170 were necessary to scavenge almost 100% of the ABTS• radicals, which also indicated the superior inhibitory effect of PRSL-150. Indeed, in the range of 5

to $30 \mu\text{g}\cdot\text{mL}^{-1}$, PRSL-150 presented a slightly higher antioxidant activity than PRSL-170. The IC_{50} of the ABTS test also followed a logarithm model ($R^2 > 0.98$), and the IC_{50} values ($\mu\text{g}\cdot\text{mL}^{-1}$) were 7.45 ± 0.08 and 8.62 ± 0.14 for PRSL-150 and PRSL-170, respectively, which were significantly different according to ANOVA ($P_{value} < 0.05$).

For comparison purposes, the IC_{50} of Trolox® in DPPH and ABTS tests were 21.83 ± 0.66 and $3.03 \pm 0.04 \mu\text{g}\cdot\text{mL}^{-1}$, respectively. Although the IC_{50} values of the PRSLs were higher than that of Trolox®, it is important to highlight that Trolox® is a synthetic water-soluble derivative of vitamin E with strong antioxidant properties [53]. Differently, PRSL is a natural molecule that was not submitted to purification or structure modification steps to improve its antioxidant performance. However, compared to IC_{50} of other lignins, such as those from sugarcane bagasse ($380 \mu\text{g}\cdot\text{mL}^{-1}$ – DPPH) [14], softwood Kraft process ($166 \mu\text{g}\cdot\text{mL}^{-1}$ – DPPH) [53], corncob (170 to $910 \mu\text{g}\cdot\text{mL}^{-1}$ – DPPH; 16 to $92 \mu\text{g}\cdot\text{mL}^{-1}$ – ABTS) [54], and wheat straw (70 to $210 \mu\text{g}\cdot\text{mL}^{-1}$ – DPPH) [55], PRSL presented better antioxidant activity (92.72 to $109.91 \mu\text{g}\cdot\text{mL}^{-1}$ – DPPH; 7.84 to $8.50 \mu\text{g}\cdot\text{mL}^{-1}$ – ABTS). The lower the IC_{50} , the higher the antioxidant power. Comparing to the lowest IC_{50} values of corncob lignin obtained in the aforementioned study [54], which performed both DPPH and ABTS tests, the lowest IC_{50} values of PRSL were 54.5% and 49.0% of those from corncob lignin for DPPH and ABTS tests, respectively. Therefore, it is

Fig. 3 Antioxidant activity of PRSL according to (a) 1,1-diphenyl-2-picrylhydrazyl (DPPH) and (b) 2,2'-Azino-bis(3-ethylbenzothiazoline-6-sulfonic acid) (ABTS) tests



possible to affirm that the PRSL has great potential as natural antioxidant for future applications.

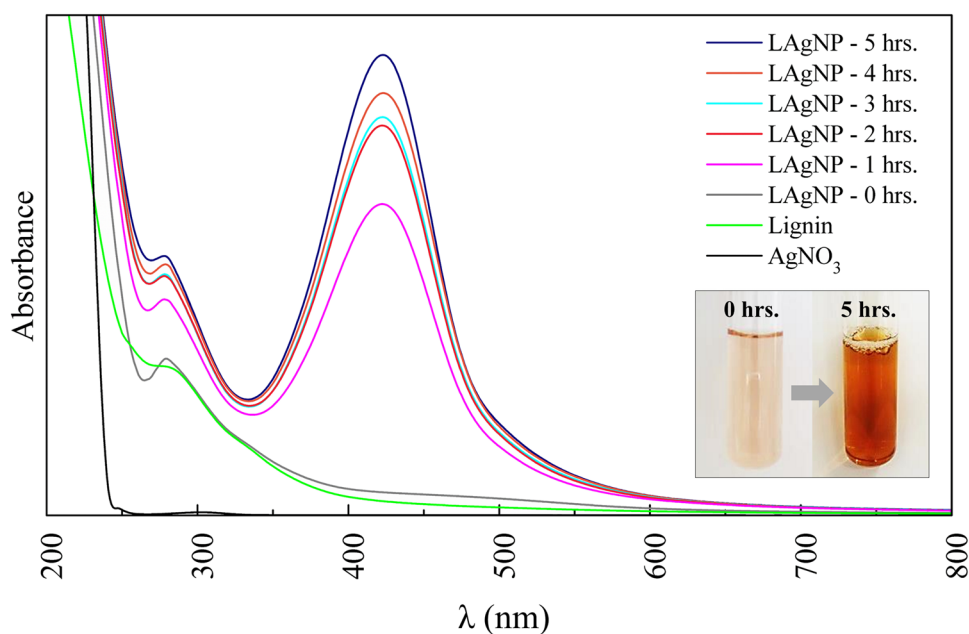
3.3 Synthesis of the LAgNPs

During the last years, some works have proposed lignin for synthesis of silver nanoparticles [2, 36, 39, 40, 45, 56–58]. However, PRSL has not yet been reported for this application, which might be an efficient way of adding value to pine residual sawdust. Therefore, considering the specific and global yields mentioned in the previous section, only PRSL-170 was utilized as reducing and stabilizing agents for LAgNPs synthesis. The metallic nanoparticles require two substances in addition to the metal precursor: a compound able to reduce the metal ions to zero-valent state, and a stabilizing agent to avoid the agglomeration of the nanoparticles, although some compounds might suffice both purposes [39, 56, 58]. In this study, the bio-reduction of LAgNPs was monitored for 5 h, as shown in Fig. 4. Another study reported that lignin-mediated silver nanoparticles synthesized at 80 °C for 4.5 h and using lignin extracted

from oil palm empty fruit bunches presented high stability in aqueous solution [36].

Lignin acted as reducing agent of silver ions producing silver nanoparticles. The reduced Ag^+ ions aggregated into silver nanoparticles whose formation was confirmed with UV–Vis by the peak around 406 nm [45]. The presence of the surface plasmon peak between 350 and 550 nm denotes the successful synthesis of silver nanoparticles, as reported in other works [36, 42, 58]. Unlike, the control sample containing only AgNO_3 showed a spectrum with no surface plasmon peak, meaning that lignin was necessary for the bio-reduction of silver ions [2]. The intensity of the surface plasmon peak of the lignin-mediated silver nanoparticles reported in this study increased with the reaction time, indicating higher amount of LAgNPs after 5 h. Additionally, the reaction solution exhibited a color change, as shown in Fig. 4, which also confirms the synthesis of silver nanoparticles [36, 42].

The FTIR spectrum of PRSL-170 is in accordance with other works [17, 40, 45, 59], as well as the LAgNPs spectrum [40, 45]. The spectra of PRSL-170 and LAgNPs are

Fig. 4 Kinetics of the LAgNPs green synthesis

presented in Fig. 5a and b, and the spectrum of LAgNPs did not present some bands that were noticed in the PRSL-170, indicating the reduction of Ag^+ ions due to lignin functional groups [40]. The band at 2952 cm^{-1} for PRSL-170, assigned to methyl and methylene groups, decreased after LAgNPs synthesis probably participating in the reduction of Ag^+ ions [40]. Both bands at 1124.89 and 1388.90 cm^{-1} might be due to C–O deformation in ester bond and symmetric bending deformation of methyl groups in the lignin structure [59, 60], caused possibly by either lignin recovery method or synthesis of LAgNPs.

Accordingly, the method for synthesizing LAgNPs in this study is in agreement with the principles of green synthesis [61]. Water was used as an eco-friendly solvent, while PRSL was proposed as a natural reducing agent and stabilizer.

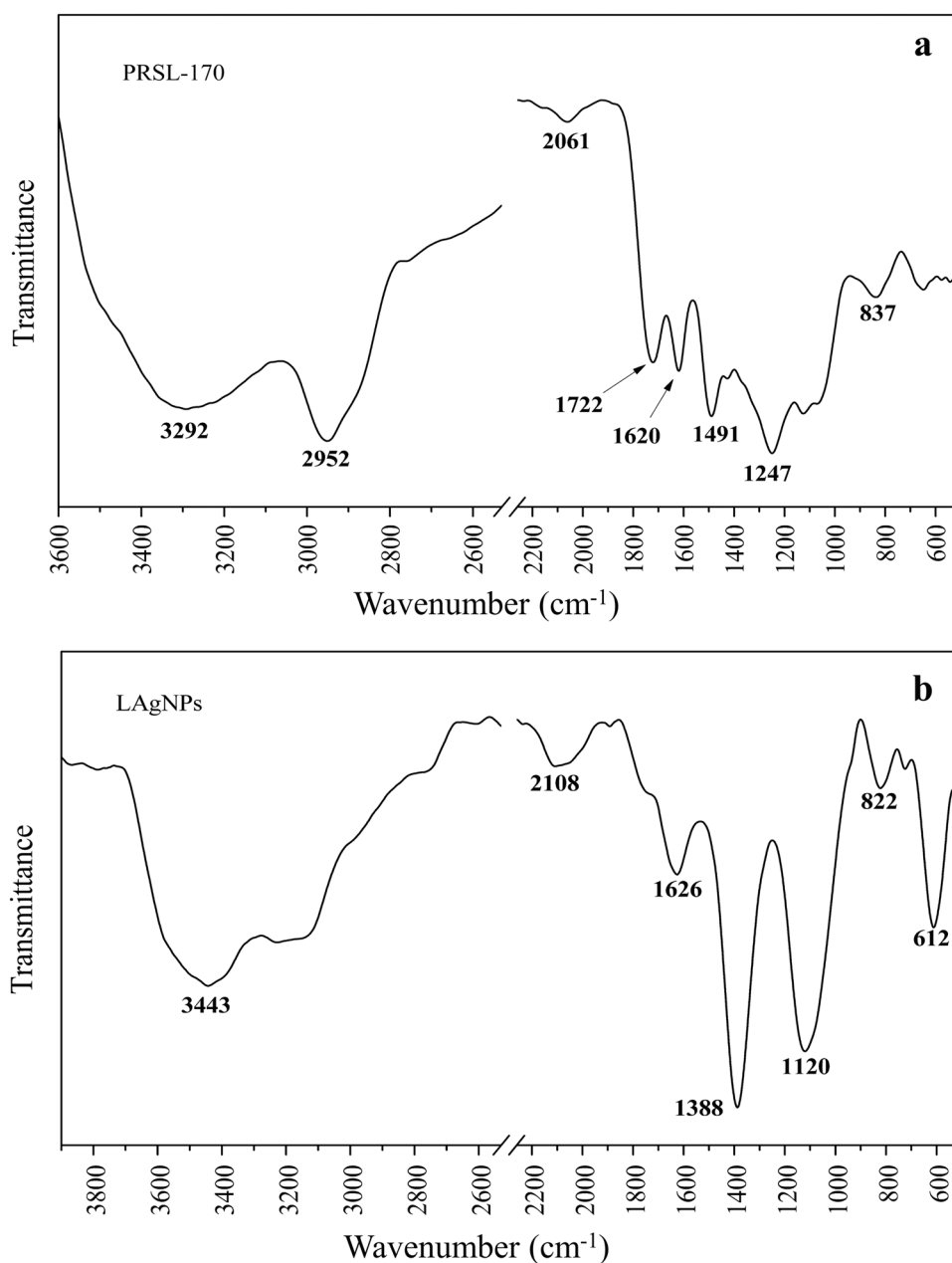
3.4 Average size and transmission electron microscopy analysis of LAgNPs

The size of the LAgNPs was analyzed by DLS. LAgNPs were a polydisperse mixture ranging in size from 7 to 100 nm and showing an average particle size of 54.18 nm. Other work also reported the synthesis of a polydisperse mixture (1 to 40 nm) of LAgNPs synthesized using lignin from oil palm empty fruit bunches [36]. The range size reported was smaller than that achieved with PRSL-170 in this study. It might be related to the type of lignin and reaction time, since that study performed the synthesis during 4.5 h, while in this study, the LAgNPs synthesis was carried out using the same concentration of reagents but for 5 h. Commercial alkali lignin from spruce was used for synthesizing LAgNPs, and their size ranged from 3 to 20 nm when

reaction time was 1 h, while narrower ranges were obtained in shorter times [2].

The TEM images are shown in Fig. 6a, b, and c, where both bright (Fig. 6a and c) and dark (Fig. 6b) field modes confirmed the formation of LAgNPs. The average particle size was 25.30 nm, and the nanoparticles exhibited a quasi-spherical morphology, as observed in Fig. 6c. The difference in the average diameter size obtained with TEM and DLS (54.18 nm) can be attributed to the fact that the measured size using DLS includes the bio-organic compounds enveloping the metallic core of nanoparticles. It is known that different techniques can report different average sizes, depending on the response of the instrument to particle number, mass, volume, or optical property [62]. Additionally, since the particle size distribution of LAgNPs is wide, in DLS, the presence of bigger particles may contribute to an increase light scattering, shifting the measured particle size towards larger values [63]. From Fig. 6a, b, and c, it can be observed that there was agglomeration of some LAgNPs, which might be related to reaction time; longer reaction times produce bigger nanoparticles [2, 56]. The synthesis of the silver nanoparticles comprises two steps: atom formation and their polymerization. The atoms in a solution are primarily reduced by the reducing agent, and then they act as nucleation centers to catalyze the reduction of the remaining metal ions. Thus, these atoms coalesce and result in metal clusters, which have their surface ions reduced again, continuing the aggregation process until high nuclearity is reached and producing larger particles [64]. Furthermore, larger particles can also be formed due to aggregation of the silver nanoparticles [39], suggesting lack of lignin either to stabilize those already formed or to reduce the Ag^+ ions

Fig. 5 Fourier-transform infrared (FTIR) spectroscopy spectra (a) before and (b) after LAgNPs green synthesis

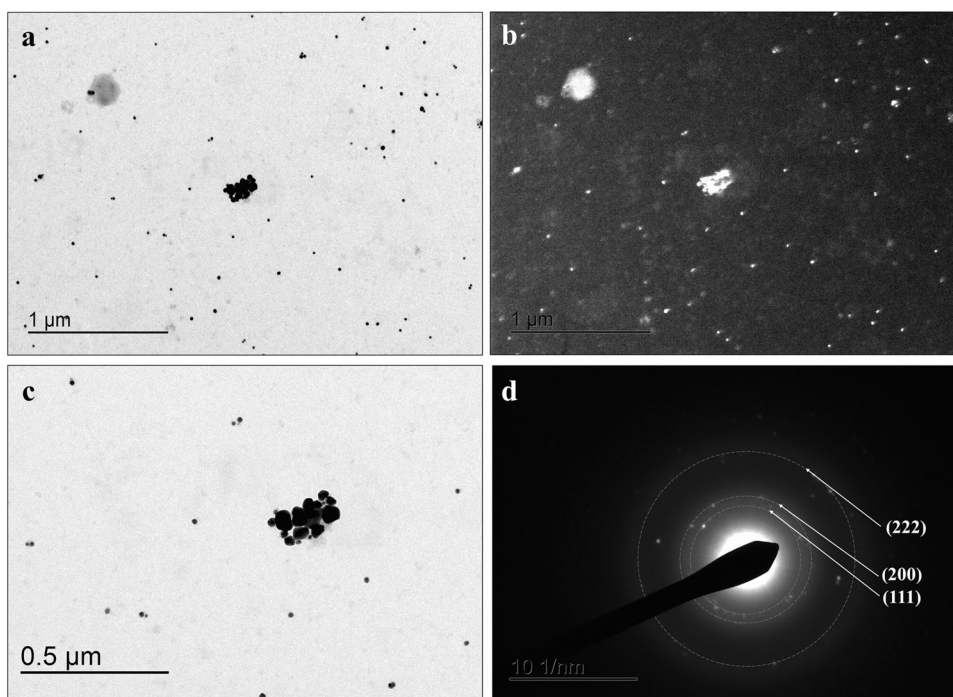


in short reaction times [2]. The methodology (chemical, physical, and biological) and conditions of the synthesis are quite related to size and shape of the nanoparticles as well [37, 65]. Other work reported the synthesis of more spherical shaped LAgNPs (diameters lower than 20 nm) at pH = 10.01, whereas LAgNPs with different shapes and sizes (diameters from 20 to 300 nm) were obtained at pH = 5.98 [2]. Furthermore, the size of the silver nanoparticles strongly influences their stability; smaller particles remain stable for months, while larger particles are more prone to sediment in a short time [58].

The SAED pattern of LAgNPs is presented in Fig. 6d. The diffraction rings, from inner to out, correspond to

(111), (200), and (222) planes according to the calculated d-spacing values [32, 33, 46]. These lattice planes suggest the face-centered-cubic (fcc) structure of silver nanoparticles, since the results are in agreement with other studies using different natural reducing agents, such as lignin from oil palm empty fruit bunches [36], *Kleinia grandiflora* leaf extract [41], *Chrysanthemum indicum* floral extract [34], *Paederia foetida* leaf extract [32], cocoa pod husk extract [42], and *Petiveria alliacea* leaf extract [43].

Fig. 6 Transmission electronic microscopic (TEM) images (a, b, and c) of bright and dark fields of the LAgNPs and (d) selected area electron diffraction (SAED)



3.5 Antibacterial activity of PRSL and LAgNPs

PRSL-170 and LAgNPs were evaluated and compared as potential antibacterial agents against Gram-positive (*Staphylococcus aureus* and *Bacillus subtilis*) and Gram-negative (*Escherichia coli* and *Salmonella typhimurium*) bacteria. As shown in Fig. 7, PRSL-170 did not exhibit a visible inhibitory effect on both Gram-positive and Gram-negative microorganisms due to the absence of dark blue color, indicating that the growth of bacteria was possible even in a medium containing 5,000 μg·mL⁻¹ of lignin. However, this

result does not suggest that lignin did not exert any inhibitory effect on the growth of the bacteria, and further studies would be required to determine the exact inhibitory percentage obtained at the concentrations evaluated.

Concerning the antimicrobial activity of lignin-mediated silver nanoparticles on bacteria, there are four well-defined mechanisms: adhesion onto the surface of cell wall and membrane, damaging these structures; penetration inside the cell, deteriorating intracellular biomolecules (proteins and DNA) and organelles (ribosomes and mitochondria); generation of reactive species and free radicals, leading to

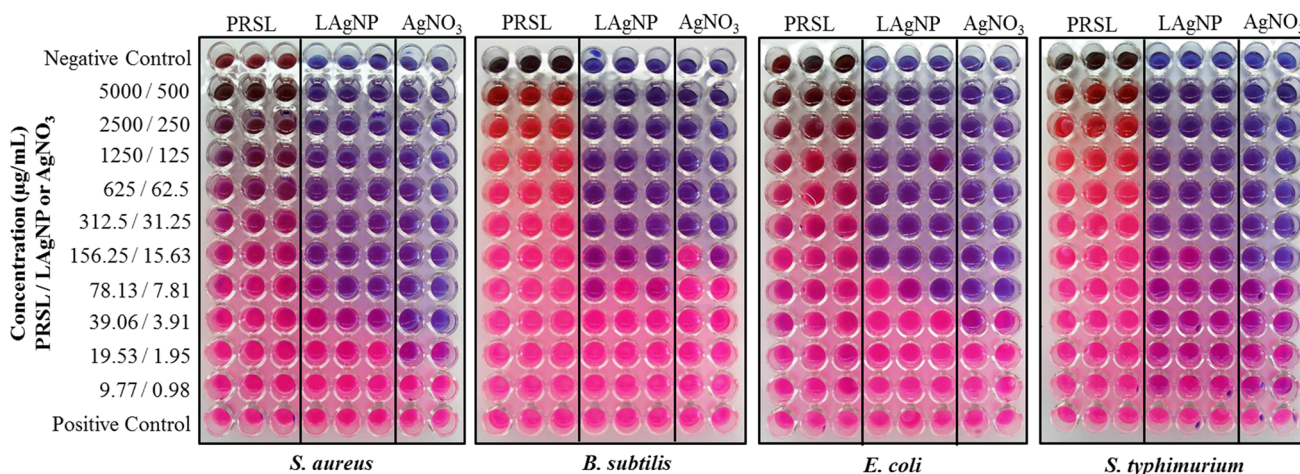


Fig. 7 Antibacterial activity of PRSL and LAgNPs against Gram-positive (*Staphylococcus aureus* and *Bacillus subtilis*) and Gram-negative (*Escherichia coli* and *Salmonella typhimurium*) bacteria

oxidative stress and cellular toxicity; and modulation of signal transduction pathway [66–68]. Therefore, silver nanoparticles with smaller size have greater antibacterial activity by easily permeating the cell wall, in addition to present larger surface area per mass, which allows higher quantities of silver atoms to reach the intracellular environment enhancing the biocidal effect [69].

The inhibition of *S. aureus* and *B. subtilis* was achieved when LAgNPs were added into the media at concentrations of 15.63 and 31.25 $\mu\text{g}\cdot\text{mL}^{-1}$, respectively. In this study, these values were named as minimum inhibitory concentration (MIC). The MIC for LAgNPs against *B. subtilis* was the same as for AgNO_3 (31.25 $\mu\text{g}\cdot\text{mL}^{-1}$), whereas against *S. aureus*, the MIC for AgNO_3 (3.91 $\mu\text{g}\cdot\text{mL}^{-1}$) was lower than that using LAgNPs (15.63 $\mu\text{g}\cdot\text{mL}^{-1}$). Silver nanoparticles are thought to interact with the cell wall of Gram-positive (*S. aureus*) bacteria and release Ag^+ cations, generating “pits” on it. Thus, those nanoparticles accumulate and start attacking the underlying layers, and the “pits” become larger, while building blocks of peptidoglycan are released [70].

The MIC for LAgNPs against *E. coli* was the same as that achieved with *S. aureus* (15.63 $\mu\text{g}\cdot\text{mL}^{-1}$). In the same way, the MIC for LAgNPs against *S. typhimurium* was equal to that obtained with *B. subtilis* (31.25 $\mu\text{g}\cdot\text{mL}^{-1}$). The MIC for AgNO_3 against both Gram-negative microorganisms was lower than the MIC of LAgNPs. A similar trend was observed in another study that also applied LAgNPs against *E. coli*, although the MIC was higher (62 $\mu\text{g}\cdot\text{mL}^{-1}$) [36]. Li and co-workers reported a higher MIC against *E. coli* using commercial silver nanoparticles (10 $\mu\text{g}\cdot\text{mL}^{-1}$) than that obtained in this study (7.81 $\mu\text{g}\cdot\text{mL}^{-1}$), which indicates that the LAgNPs produced in this study achieved better results [71]. The outer membrane of Gram-negative bacteria is a lipid bilayer whose inner leaflet mostly contains phospholipid chains, whereas the outer leaflet has lipopolysaccharide molecules. In *E. coli*, silver nanoparticles cause the leakage of reducing sugars and proteins, and inside the cell, they disturb the activity of respiratory chain dehydrogenases [71, 72]. By way of comparison with commercial antibiotics, the MIC of ampicillin and kanamycin against *S. aureus* is 0.25 $\mu\text{g}\cdot\text{mL}^{-1}$ and 8 $\mu\text{g}\cdot\text{mL}^{-1}$, respectively, whereas the MIC against *E. coli* is 32 $\mu\text{g}\cdot\text{mL}^{-1}$ for both mentioned antibiotics [73].

The results indicated that LAgNPs and AgNO_3 presented almost the same antibacterial effect, since LAgNPs did not show lower MIC values than AgNO_3 . It might be related to the aggregation of the LAgNPs as previously mentioned. The smaller the nanoparticle, the higher its surface to volume ratio, which would allow it to interact with bacteria as compared to the same concentration of larger counterparts. Small-size silver nanoparticles present higher solubility, which improves their oxidation to easily release Ag^+ cations, enhancing their antibacterial effect. However, when aggregation occurs, the effect

will probably be the same as the larger silver particles [67]. Furthermore, it must be pointed out that most of the AgNO_3 is in ionic or soluble complex form in the MHB medium, readily available for interacting with microorganisms and causing faster effects on them [36, 74]. Conversely, silver nanoparticles are well-known slow-release devices of silver ions over time, which presents the advantage of prolonging the antibacterial effect [75, 76]. Accordingly, there is a difference in the action mechanisms of silver ions and silver nanoparticles [77, 78]. Factors such as size, shape, and surface charge of silver nanoparticles, in addition to ionic strength and composition of the medium, influence their stability and biological activities [79]. LAgNPs might present negative charge as well as bacteria cell wall, hindering the interaction between them. Differently, the available Ag^+ cations from AgNO_3 easily interact with bacteria by strong ionic attraction, producing the antibacterial effect faster [80]. In order to enhance the antibacterial activity of LAgNPs, a positive capping agent might have been used, since it would avoid agglomeration of the LAgNPs [67] and facilitate the electrostatic attraction between the negatively charged bacterial cell wall and LAgNPs [81].

Conclusively, the tests performed in this study were able to show that PRSL is capable of synthesizing LAgNPs with promising antibacterial properties, since lignin alone did not visibly inhibit the growth of Gram-positive and Gram-negative bacteria. Possibly, higher antibacterial activity of LAgNPs would have been achieved if a capping agent was used or the surface of the particles was modified. Besides, it is worth noting that PRSL utilization in this green synthesis also contributed producing silver nanoparticles with fewer impacts on the environment than traditional chemical methods. Moreover, the use of PRSL for value-added applications such as silver nanoparticles can contribute to increase the feasibility of a biorefinery. In that regard, it is also important to keep in mind that these nanoparticles have the potential to be applied in other different fields [37]. Currently, silver nanoparticles are used due to their antiseptic properties in coatings, keyboards, washing machines, air conditioners, wound dressings, and biomedical devices [29, 82, 83]. Furthermore, the utilization of lignin in the synthesis of silver nanoparticles presents advantages compared to other green approaches, such as plant extracts and microorganisms. Plant extracts are less resistant to higher temperatures than lignin, which is also easier to recover than microorganisms that require proper procedures during their manipulation [36].

4 Conclusions

The wood processing in sawmills produces large amounts of pine residual sawdust, a byproduct considered waste. In this study, three lignins obtained from pine residual sawdust (PRSL-130, PRSL-150, and PRSL-170) had their

antioxidant activity evaluated by DPPH and ABTS tests. The great capacity of PRSL as a natural antioxidant was proved by both methods, and it is intrinsically related to the total phenolic content. PRSL-170 was chosen to be used in the green synthesis of silver nanoparticles. Although it was not possible to determine a MIC for PRSL, LAgNPs demonstrated antibacterial effect against Gram-positive (*Staphylococcus aureus* and *Bacillus subtilis*) and Gram-negative (*Escherichia coli* and *Salmonella typhimurium*) bacteria. The results suggested that the LAgNPs can be an efficient antibacterial agent. Aggregation of LAgNPs was observed; however, other methodologies can be performed in future researches to circumvent this drawback. Nevertheless, the results showed the potential of PRSL as an antioxidant agent as well as for green synthesis of silver nanoparticles with high potential for antibacterial applications. Furthermore, the utilization of pine residual sawdust, a renewable resource, contributes to its valorization and stimulates the feasibility of a biorefinery in the wood industry, avoiding environmental problems for improper disposal of wastes.

Author contribution Not applicable.

Availability of data and material Not applicable.

Code availability Not applicable.

Declarations

Conflict of interest The authors declare no competing interests.

References

- Okolie JA, Nanda S, Dalai AK, Kozinski JA (2020) Chemistry and specialty industrial applications of lignocellulosic biomass. *Waste Biomass Valoriz.* <https://doi.org/10.1007/s12649-020-01123-0>
- Hu S, Lo HY (2016) Silver nanoparticle synthesis using lignin as reducing and capping agents: a kinetic and mechanistic study. *Int J Biol Macromol* 82:856–862. <https://doi.org/10.1016/j.ijbiomac.2015.09.066>
- Calvo-Flores FG, Dobado JA, Isac-García J, Martín-Martínez FJ (2015) Background and overview. In: *Lignin and lignans as renewable raw materials: Chemistry, technology and applications*, 1st edn. John Wiley & Sons, Ltd., p 8. <https://doi.org/10.1002/9781118682784.ch1>
- Espinoza-Acosta JL, Torres-Chávez PI, Ramírez-Wong B et al (2016) Antioxidant, antimicrobial, and antimutagenic properties of technical lignins and their applications. *BioResources* 11:5452–5481. https://doi.org/10.15376/biores.11.2.Espinoza_Acosta
- García A, Toledano A, Andrés MÁ, Labidi J (2010) Study of the antioxidant capacity of *Miscanthus sinensis* lignins. *Process Biochem* 45:935–940. <https://doi.org/10.1016/j.procbio.2010.02.015>
- Karavalakis G, Hilari D, Givalou L et al (2011) Storage stability and ageing effect of biodiesel blends treated with different antioxidants. *Energy* 36:369–374. <https://doi.org/10.1016/J.ENERGY.2010.10.029>
- Jakeria MR, Fazal MA, Haseeb ASMA (2014) Influence of different factors on the stability of biodiesel: a review. *Renew Sustain Energy Rev* 30:154–163. <https://doi.org/10.1016/J.RSER.2013.09.024>
- Wise Guy Reports (2019) Global rubber antioxidant market insights, Forecast to 2025– WiseGuyReports
- Markets and Markets (2019) Plastic antioxidants Market worth 2.11 Billion USD by 2022
- An L, Wang G, Jia H et al (2017) Fractionation of enzymatic hydrolysis lignin by sequential extraction for enhancing antioxidant performance. *Int J Biol Macromol* 99:674–681. <https://doi.org/10.1016/j.ijbiomac.2017.03.015>
- Kai D, Tan MJ, Chee PL et al (2016) Towards lignin-based functional materials in a sustainable world. *Green Chem* 18:1175–1200. <https://doi.org/10.1039/c5gc02616d>
- Jiang B, Zhang Y, Gu L et al (2018) Structural elucidation and antioxidant activity of lignin isolated from rice straw and alkali-oxygen black liquor. *Int J Biol Macromol* 116:513–519. <https://doi.org/10.1016/j.ijbiomac.2018.05.063>
- García A, Giorgia S, Jalel L (2017) Antioxidant and biocide behaviour of lignin fractions from apple tree pruning residues. *Ind Crop Prod J* 104:242–252. <https://doi.org/10.1007/978-1-4939-1447-0>
- Kaur R, Uppal SK, Sharma P (2017) Antioxidant and antibacterial activities of sugarcane bagasse lignin and chemically modified lignins. *Sugar Tech* 19:675–680. <https://doi.org/10.1007/s12355-017-0513-y>
- Coral Medina DJ, Lorenci Woiciechowski A, Zandona Filho A et al (2016) Biological activities and thermal behavior of lignin from oil palm empty fruit bunches as potential source of chemicals of added value. *Ind Crop Prod* 94:630–637. <https://doi.org/10.1016/j.indcrop.2016.09.046>
- Ma P, Gao Y, Zhai H (2013) Fractionated wheat straw lignin and its application as antioxidant. *BioResources* 8:5581–5595. <https://doi.org/10.15376/biores.8.4.5581-5595>
- Cavali M, Ricardo Soccol C, Tavares D et al (2020) Effect of sequential acid-alkaline treatment on physical and chemical characteristics of lignin and cellulose from pine (*Pinus* spp.) residual sawdust. *Bioresour Technol* 316:123884. <https://doi.org/10.1016/j.biortech.2020.123884>
- Bravo C, Garcés D, Faba L et al (2017) Selective arabinose extraction from *Pinus* sp. sawdust by two-step soft acid hydrolysis. *Ind Crop Prod* 104:229–236. <https://doi.org/10.1016/j.indcrop.2017.04.027>
- Ogunwusi A (2014) Wood waste generation in the forest industry in Nigeria and prospects for its industrial utilization. *Civ Environ Res* 6:62–70
- Vega LY, López L, Valdés CF, Chejne F (2019) Assessment of energy potential of wood industry wastes through thermochemical conversions. *Waste Manag* 87:108–118. <https://doi.org/10.1016/J.WASMAN.2019.01.048>
- Schneider VE, Peresin D, Andréia Cristina Trentin Taison AB, Sambuichi RHR (2012) Diagnóstico dos Resíduos Orgânicos do Setor Agrossilvopastoril e Agroindústrias Associadas. *Inst Pesqui Econômica Apl – IPEA* 134
- European Organization of the Sawmill Industry (2020) Building a green future - Annual Report 2019–2020
- Rominyi OL, Adaramola BA, Ikumapayi OM et al (2017) Potential utilization of sawdust in energy, manufacturing and agricultural industry; waste to wealth. *World J Eng Technol* 05:526–539. <https://doi.org/10.4236/wjet.2017.53045>
- Saif S, Tahir A, Chen Y (2016) Green synthesis of iron nanoparticles and their environmental applications and implications. *Nanomaterials* 6:209. <https://doi.org/10.3390/nano6110209>

25. Akbari A, Amini M, Tarassoli A et al (2018) Transition metal oxide nanoparticles as efficient catalysts in oxidation reactions. *Nano-Structures & Nano-Objects* 14:19–48. <https://doi.org/10.1016/J.NANOSO.2018.01.006>
26. Niska K, Zielinska E, Radomski MW, Inkielawicz-Stepniak I (2018) Metal nanoparticles in dermatology and cosmetology: interactions with human skin cells. *Chem Biol Interact* 295:38–51. <https://doi.org/10.1016/J.CBI.2017.06.018>
27. Garcia CV, Shin GH, Kim JT (2018) Metal oxide-based nanocomposites in food packaging: applications, migration, and regulations. *Trends Food Sci Technol* 82:21–31. <https://doi.org/10.1016/J.TIFS.2018.09.021>
28. Elegbede JA, Lateef A (2019) Green synthesis of silver (Ag), gold (Au), and silver–gold (Ag–Au) alloy nanoparticles: a review on recent advances, trends, and biomedical applications. In: *Nanotechnology and nanomaterial applications in food, health, and biomedical sciences*, 1st ed., p 87. Published 2015 by Apple Academic Press Inc. <https://doi.org/10.1201/9780429425660-1>
29. Singh A, Kaur K (2019) Biological and physical applications of silver nanoparticles with emerging trends of green synthesis. *Silver Nanoparticles - Heal Saf* [Working Title]. <https://doi.org/10.5772/intechopen.88684>
30. Beyene HD, Werkneh AA, Bezabh HK, Ambaye TG (2017) Synthesis paradigm and applications of silver nanoparticles (AgNPs), a review. *Sustain Mater Technol* 13:18–23. <https://doi.org/10.1016/j.susmat.2017.08.001>
31. Barabadi H, Tajani B, Moradi M et al (2019) Penicillium family as emerging nanofactory for biosynthesis of green nanomaterials: a journey into the world of microorganisms. *J Clust Sci* 30:843–856. <https://doi.org/10.1007/s10876-019-01554-3>
32. Mollick MMR, Bhowmick B, Maity D et al (2012) Green synthesis of silver nanoparticles using *Paederia foetida* L. leaf extract and assessment of their antimicrobial activities. *Int J Green Nanotechnol Biomed* 4:230–239. <https://doi.org/10.1080/19430892.2012.706103>
33. Ananda Murthy HC, DesalegnZeleke T, Ravikumar CR et al (2020) Electrochemical properties of biogenic silver nanoparticles synthesized using *Hagenia abyssinica* (Brace) JF. Gmel. medicinal plant leaf extract. *Mater Res Express* 7:055016. <https://doi.org/10.1088/2053-1591/ab9252>
34. Arokiyaraj S, Dinesh Kumar V, Elakya V et al (2015) Biosynthesized silver nanoparticles using floral extract of *Chrysanthemum indicum* L.—potential for malaria vector control. *Environ Sci Pollut Res* 22:9759–9765. <https://doi.org/10.1007/s11356-015-4148-9>
35. Adelere IA, Lateef A (2011) Novel approach to the green synthesis of metallic nanoparticles: the use of agro-wastes, enzymes and pigments. *Nanotechnol Rev* 5:42. <https://doi.org/10.1515/ntrev-2016-0024>
36. Zevallos Torres LA, Woiciechowski AL, de Andrade O, Tanobe V et al (2021) Lignin from oil palm empty fruit bunches: characterization, biological activities and application in green synthesis of silver nanoparticles. *Int J Biol Macromol* 167:1499–1507. <https://doi.org/10.1016/j.ijbiomac.2020.11.104>
37. Syafiuddin A, Salmiati SMR et al (2017) A review of silver nanoparticles: research trends, global consumption, synthesis, properties, and future challenges. *J Chinese Chem Soc* 64:732–756. <https://doi.org/10.1002/jccs.201700067>
38. Peng H, Guo H, Gao P et al (2021) Reduction of silver ions to silver nanoparticles by biomass and biochar: mechanisms and critical factors. *Sci Total Environ* 779:146326. <https://doi.org/10.1016/j.scitotenv.2021.146326>
39. Milczarek G, Rebis T, Fabianska J (2013) Colloids and surfaces b: biointerfaces one-step synthesis of lignosulfonate-stabilized silver nanoparticles. *Colloids Surfaces B Biointerfaces* 105:335–341. <https://doi.org/10.1016/j.colsurfb.2013.01.010>
40. Aadil KR, Barapatre A, Meena AS, Jha H (2016) Hydrogen peroxide sensing and cytotoxicity activity of Acacia lignin stabilized silver nanoparticles. *Int J Biol Macromol* 82:39–47. <https://doi.org/10.1016/j.ijbiomac.2015.09.072>
41. Kanagamani K, Muthukrishnan P, Shankar K et al (2019) Antimicrobial, cytotoxicity and photocatalytic degradation of norfloxacin using *Kleinia grandiflora* mediated silver nanoparticles. *J Clust Sci* 30:1415–1424. <https://doi.org/10.1007/s10876-019-01583-y>
42. Lateef A, Azeed MA, Asafa TB et al (2016) Cocoa pod husk extract-mediated biosynthesis of silver nanoparticles: its antimicrobial, antioxidant and larvicidal activities. *J Nanostructure Chem* 6:159–169. <https://doi.org/10.1007/s40097-016-0191-4>
43. Lateef A, Folarin BI, Oladejo SM et al (2018) Characterization, antimicrobial, antioxidant, and anticoagulant activities of silver nanoparticles synthesized from *Petiveria alliacea* L. leaf extract. *Prep Biochem Biotechnol* 48:646–652. <https://doi.org/10.1080/10826068.2018.1479864>
44. Klapiszewski TR, M. K, et al (2015) Kraft lignin/silica-AgNPs as a functional material with antibacterial activity. *Colloids Surfaces B Biointerfaces* 134:220–228. <https://doi.org/10.1016/j.colsurfb.2015.06.056>
45. Marulasiddeshwara MB, Dakshayani SS, Sharath Kumar MN et al (2017) Facile-one pot-green synthesis, antibacterial, antifungal, antioxidant and antiplatelet activities of lignin capped silver nanoparticles: a promising therapeutic agent. *Mater Sci Eng C* 81:182–190. <https://doi.org/10.1016/j.msec.2017.07.054>
46. Vishwajeet S, Ankita S, Nitin W (2015) Biosynthesis of silver nanoparticles by plants crude extracts and their characterization using UV, XRD, TEM and EDX. *African J Biotechnol* 14:2554–2567. <https://doi.org/10.5897/ajb2015.14692>
47. Balouiri M, Sadiki M, Ibsouda SK (2016) Methods for in vitro evaluating antimicrobial activity: a review. *J Pharm Anal* 6:71–79. <https://doi.org/10.1016/j.jpha.2015.11.005>
48. Karuppusamy S, Rajasekaran KM (2009) High throughput antibacterial screening of plant extracts by resazurin redox with special reference to medicinal plants of Western Ghats. *Glob J Pharmacol* 3:63–68
49. O'Brien J, Ian W, Terry O, François P (2000) Investigation of the Alamar Blue (resazurin) fluorescent dye for the assessment of mammalian cell cytotoxicity. *Eur J Biochem* 267:5421–5426
50. Teh CH, Nazni WA, Nurulhusna AH et al (2017) Determination of antibacterial activity and minimum inhibitory concentration of larval extract of fly via resazurin-based turbidometric assay. *BMC Microbiol* 17:1–8. <https://doi.org/10.1186/s12866-017-0936-3>
51. Azadi P, Inderwildi OR, Farnood R, King DA (2013) Liquid fuels, hydrogen and chemicals from lignin: a critical review. *Renew Sustain Energy Rev* 21:506–523. <https://doi.org/10.1016/j.rser.2012.12.022>
52. García A, González Alriols M, Spigno G, Labidi J (2012) Lignin as natural radical scavenger. Effect of the obtaining and purification processes on the antioxidant behaviour of lignin. *Biochem Eng J* 67:173–185. <https://doi.org/10.1016/j.bej.2012.06.013>
53. Sadeghifar H, Argyropoulos DS (2015) Correlations of the antioxidant properties of softwood Kraft lignin fractions with the thermal stability of its blends with polyethylene. *ACS Sustain Chem Eng* 3:349–356. <https://doi.org/10.1021/sc500756n>
54. Michelin M, Liebenritt S, Vicente AA, Teixeira JA (2018) Lignin from an integrated process consisting of liquid hot water and ethanol organosolv: physicochemical and antioxidant properties. *Int J Biol Macromol* 120:159–169. <https://doi.org/10.1016/j.ijbiomac.2018.08.046>
55. Sun S, Liu F, Zhang L, Fan X (2018) One-step process based on the order of hydrothermal and alkaline treatment for producing

- lignin with high yield and antioxidant activity. *Ind Crops Prod* 119:260–266. <https://doi.org/10.1016/j.indcrop.2018.04.030>
56. Hu S, Lo HY (2015) Synthesis of surface bound silver nanoparticles on cellulose fibers using lignin as multi-functional agent. *Carbohydr Polym* 131:134–141. <https://doi.org/10.1016/j.carbpol.2015.05.060>
 57. Xue Y, Qiu X, Liu Z, Li Y (2018) Facile and efficient synthesis of silver nanoparticles based on biorefinery wood lignin and its application as the optical sensor. *ACS Sustain Chem Eng* 6:7695–7703. <https://doi.org/10.1021/acsschemeng.8b00578>
 58. Modrzejewska-Sikorska A, Konował E, Cichy A et al (2017) The effect of silver salts and lignosulfonates in the synthesis of lignosulfonate-stabilized silver nanoparticles. *J Mol Liq* 240:80–86. <https://doi.org/10.1016/j.molliq.2017.05.065>
 59. Lourençon TV, Hansel FA, Da Silva TA et al (2015) Hardwood and softwood Kraft lignins fractionation by simple sequential acid precipitation. *Sep Purif Technol* 154:82–88. <https://doi.org/10.1016/j.seppur.2015.09.015>
 60. Huang Y, Liu H, Yuan H et al (2018) Association of chemical structure and thermal degradation of lignins from crop straw and softwood. *J Anal Appl Pyrolysis* 134:25–34. <https://doi.org/10.1016/j.jaap.2018.04.008>
 61. Mohan S, Oluwafemi OS, George SC et al (2014) Completely green synthesis of dextrose reduced silver nanoparticles, its antimicrobial and sensing properties. *Carbohydr Polym* 106:469–474. <https://doi.org/10.1016/j.carbpol.2014.01.008>
 62. Sujitha MV, Kannan S (2013) Green synthesis of gold nanoparticles using citrus fruits (*Citrus limon*, *Citrus reticulata* and *Citrus sinensis*) aqueous extract and its characterization. *Spectrochim Acta Part A Mol Biomol Spectrosc* 102:15–23. <https://doi.org/10.1016/j.saa.2012.09.042>
 63. Souza TGF, Ciminelli VST, Mohallem NDS (2016) A comparison of TEM and DLS methods to characterize size distribution of ceramic nanoparticles. *J Phys Conf Ser* 733:012039. <https://doi.org/10.1088/1742-6596/733/1/012039>
 64. Pandey S, Goswami GK, Nanda KK (2012) Green synthesis of biopolymer–silver nanoparticle nanocomposite: an optical sensor for ammonia detection. *Int J Biol Macromol* 51:583–589. <https://doi.org/10.1016/j.jbiomac.2012.06.033>
 65. Dhand C, Dwivedi N, Loh XJ et al (2015) Methods and strategies for the synthesis of diverse nanoparticles and their applications: a comprehensive overview. *RSC Adv* 5:105003–105037. <https://doi.org/10.1039/c5ra19388e>
 66. Dakal TC, Kumar A, Majumdar RS, Yadav V (2016) Mechanistic basis of antimicrobial actions of silver nanoparticles. *Front Microbiol* 7:1–17. <https://doi.org/10.3389/fmicb.2016.01831>
 67. Zheng K, Setyawati MI, Leong DT, Xie J (2018) Antimicrobial silver nanomaterials. *Coord Chem Rev* 357:1–17. <https://doi.org/10.1016/j.ccr.2017.11.019>
 68. Klapiszewski Ł, Rzemieniecki T, Krawczyk M et al (2015) Kraft lignin/silica-AgNPs as a functional material with antibacterial activity. *Colloids Surfaces B Biointerfaces* 134:220–228. <https://doi.org/10.1016/j.colsurfb.2015.06.056>
 69. Van Dong P, Ha C, Binh L, Kasbohm J (2012) Chemical synthesis and antibacterial activity of novel-shaped silver nanoparticles. *Int Nano Lett* 2:9. <https://doi.org/10.1186/2228-5326-2-9>
 70. Mirzajani F, Ghassempour A, Aliahmadi A, Esmaeili MA (2011) Antibacterial effect of silver nanoparticles on *Staphylococcus aureus*. *Res Microbiol* 162:542–549. <https://doi.org/10.1016/j.resmic.2011.04.009>
 71. Li WR, Xie XB, Shi QS et al (2010) Antibacterial activity and mechanism of silver nanoparticles on *Escherichia coli*. *Appl Microbiol Biotechnol* 85:1115–1122. <https://doi.org/10.1007/s00253-009-2159-5>
 72. Sondi I, Salopek-Sondi B (2004) Silver nanoparticles as antimicrobial agent: a case study on *E. coli* as a model for Gram-negative bacteria. *J Colloid Interface Sci* 275:177–182. <https://doi.org/10.1016/j.jcis.2004.02.012>
 73. Garza-Cervantes JA, Meza-Bustillos JF, Resendiz-Hernández H et al (2020) Re-sensitizing ampicillin and kanamycin-resistant *E. coli* and *S. aureus* using synergistic metal micronutrients-antibiotic combinations. *Front Bioeng Biotechnol* 8:1–21. <https://doi.org/10.3389/fbioe.2020.00612>
 74. Zhang S, Liu L, Pareek V et al (2014) Effects of broth composition and light condition on antimicrobial susceptibility testing of ionic silver. *J Microbiol Methods* 105:42–46. <https://doi.org/10.1016/j.mimet.2014.07.009>
 75. Greulich C, Kittler S, Epple M et al (2009) Studies on the biocompatibility and the interaction of silver nanoparticles with human mesenchymal stem cells (hMSCs). *Langenbeck's Arch Surg* 394:495–502. <https://doi.org/10.1007/s00423-009-0472-1>
 76. Comfort KK, Maurer EI, Hussain SM (2014) Slow release of ions from internalized silver nanoparticles modifies the epidermal growth factor signaling response. *Colloids Surfaces B Biointerfaces* 123:136–142. <https://doi.org/10.1016/j.colsurfb.2014.09.008>
 77. Kędziora A, Speruda M, Krzyżewska E et al (2018) Similarities and differences between silver ions and silver in nanoforms as antibacterial agents. *Int J Mol Sci* 19:444. <https://doi.org/10.3390/ijms19020444>
 78. Mosselhy DA, El-Aziz MA, Hanna M et al (2015) Comparative synthesis and antimicrobial action of silver nanoparticles and silver nitrate. *J Nanoparticle Res* 17:1–10. <https://doi.org/10.1007/s11051-015-3279-8>
 79. Reidy B, Haase A, Luch A et al (2013) Mechanisms of silver nanoparticle release, transformation and toxicity: a critical review of current knowledge and recommendations for future studies and applications. *Materials (Basel)* 6:2295–2350. <https://doi.org/10.3390/ma6062295>
 80. Zhang Y, Peng H, Huang W et al (2008) Facile preparation and characterization of highly antimicrobial colloid Ag or Au nanoparticles. *J Colloid Interface Sci* 325:371–376. <https://doi.org/10.1016/j.jcis.2008.05.063>
 81. Richter AP, Brown JS, Bharti B et al (2015) An environmentally benign antimicrobial nanoparticle based on a silver-infused lignin core. *Nat Nanotechnol* 10:817–823. <https://doi.org/10.1038/nnano.2015.141>
 82. Oldenburg SJ, Saunders AE (2021) Silver nanomaterials for biological applications. Merck Group. Available from: <https://www.sigmaaldrich.com/BR/pt/technical-documents/technical-article/materials-science-and-engineering/biosensors-and-imaging/silver-nanomaterials>
 83. Chauret CP (2014) Sanitization. *Encycl Food Microbiol Second Ed* 3:360–364. <https://doi.org/10.1016/B978-0-12-384730-0.00407-9>

Publisher's note Springer Nature remains neutral with regard to jurisdictional claims in published maps and institutional affiliations.